

1 **Using Core Genome Alignments to Assign Bacterial Species**

2

3 Matthew Chung<sup>a,b</sup>, James B. Munro<sup>a</sup>, Julie C. Dunning Hotopp<sup>a,b,c</sup>#

4 <sup>a</sup> Institute for Genome Sciences, University of Maryland Baltimore, Baltimore, MD 21201, USA

5 <sup>b</sup> Department of Microbiology and Immunology, University of Maryland Baltimore, Baltimore, MD

6 21201, USA

7 <sup>c</sup> Greenebaum Comprehensive Cancer Center, University of Maryland Baltimore, Baltimore, MD 21201,

8 USA

9

10 Running Title: Core Genome Alignments to Assign Bacterial Species

11

12 #Address correspondence to Julie C. Dunning Hotopp, [jdhottopp@som.umaryland.edu](mailto:jdhottopp@som.umaryland.edu).

13

14 Word count Abstract: 371 words

15 Word count Text: 4,833 words

16

17 **ABSTRACT**

18 With the exponential increase in the number of bacterial taxa with genome sequence data, a new  
19 standardized method is needed to assign bacterial species designations using genomic data that is  
20 consistent with the classically-obtained taxonomy. This is particularly acute for unculturable obligate  
21 intracellular bacteria like those in the Rickettsiales, where classical methods like DNA-DNA hybridization  
22 cannot be used to define species. Within the Rickettsiales, species designations have been applied  
23 inconsistently, often obfuscating the relationship between organisms and the context for experimental  
24 results. In this study, we generated core genome alignments for a wide range of genera with classically  
25 defined species, including *Arcobacter*, *Caulobacter*, *Erwinia*, *Neisseria*, *Polaribacter*, *Ralstonia*, *Thermus*,  
26 as well as genera within the Rickettsiales including *Rickettsia*, *Orientia*, *Ehrlichia*, *Neoehrlichia*,  
27 *Anaplasma*, *Neorickettsia*, and *Wolbachia*. A core genome alignment sequence identity (CGASI)  
28 threshold of 96.8% was found to maximize the prediction of classically-defined species. Using the CGASI  
29 cutoff, the *Wolbachia* genus can be delineated into species that differ from the currently used  
30 supergroup designations, while the *Rickettsia* genus is delineated into nine species, as opposed to the  
31 current 27 species. Additionally, we find that core genome alignments cannot be constructed between  
32 genomes belonging to different genera, establishing a bacterial genus cutoff that suggests the need to  
33 create new genera from the *Anaplasma* and *Neorickettsia*. By using core genome alignments to assign  
34 taxonomic designations, we aim to provide a high-resolution, robust method for bacterial nomenclature  
35 that is aligned with classically-obtained results.

36 **IMPORTANCE**

37 With the increasing availability of genome sequences, we sought to develop and apply a robust, high-  
38 resolution method for the assignment of genera and species designations that can recapitulate  
39 classically-defined taxonomic designations. We developed genera and species cutoffs using both the  
40 length and sequence identity of core genome alignments as taxonomic criteria, respectively. These

41 criteria were then tested on diverse bacterial genera with an emphasis on the taxonomy of organisms  
42 within the order Rickettsiales, where species designations have been applied inconsistently. Our results  
43 indicate that the *Rickettsia* have an overabundance of species designations and that there are clear  
44 demarcations of *Wolbachia* species that do not align precisely with the existing supergroup  
45 designations. Lastly, we find that the current *Anaplasma* and *Neorickettsia* genus designations are both  
46 too broad and need to be divided.

47 **INTRODUCTION**

48 While acknowledging the disdain some scientists have for taxonomy, Stephen Jay Gould frequently  
49 highlighted in his writings how the classifications arising from a good taxonomy both reflects and directs  
50 our thinking, stating, “the way we order reflects the way we think. Historical changes in classification are  
51 the fossilized indicators of conceptual revolutions” (1). Historically, bacterial species delimitation relied  
52 on the phenotypic, morphological, and chemotaxonomic characterization (2-4). The 1960s saw the  
53 introduction of molecular techniques in bacterial species delimitation through the use of GC-content (5),  
54 DNA-DNA hybridization (6), and 16S rRNA sequencing (7, 8). Currently, databases like SILVA (9) and  
55 Greengenes (10) use 16S rRNA sequencing to identify bacteria. However, 16S rRNA sequencing often  
56 fails to separate closely-related taxa, and its utility for species-level identification is questionable (10-  
57 12). Multilocus sequence analysis (MLSA) has also been used to determine species (13), as has  
58 phylogenetic analysis of both rRNA and protein-coding genes (3, 14, 15). Non-genomic mass-  
59 spectrometry-based approaches, in which expressed proteins and peptides are characterized, provide  
60 complementary data to phenotypic and genomic species delimitations (16, 17) and are used in clinical  
61 microbiology laboratories. However, DNA-DNA hybridization (DDH) remains the “gold standard” of  
62 defining bacterial species (18, 19), despite its inability to address non-culturable organisms and the  
63 intensive labor involved that limits its applicability. A new genome-based bacterial species definition is  
64 attractive given the increasing availability of bacterial genomes, rapid sequencing improvements with  
65 decreasing sequencing costs, and data standards and databases that enable data sharing.

66 Average nucleotide identity (ANI) and *in silico* DDH were developed as genomic era tools that allow for  
67 bacterial classification with a high correlation to results obtained using wet lab DDH, while bypassing the  
68 associated difficulties (20-22). For ANI calculations, the genome of the query organism is split into 1 kbp  
69 fragments, which are then searched against the whole genome of a reference organism. The average  
70 sequence identity of all matches having >60% overall sequence identity over >70% of their length is

71 defined as the ANI between the two organisms (18). *In silico* DDH, also referred to as digital DDH  
72 (dDDH), uses the sequence similarity of conserved regions between the genomes of interests, such as  
73 high scoring segment pairs (HSPs) or maximally unique matches (MUMs) (23), to calculate genome-to-  
74 genome distances. These distances are converted to a dDDH value, which is intended to be analogous to  
75 DDH values obtained using traditional laboratory methods. There are three formulas for calculating  
76 dDDH values between two genomes using either (1) the length of all HSPs divided by the total genome  
77 length, (2) the sum of all identities found in HSPs divided by the overall HSP length, and (3) the sum of all  
78 identities found in HSPs divided by the total genome length, with the second formula being  
79 recommended for assigning species designations for draft genomes (24, 25). However, these methods  
80 do not report the total length of fragments that match the reference genome, and problems arise when  
81 only a small number of fragments are unknowingly used.

82 Recent phylogenomic analyses have shifted towards using the core proteome, a concatenated alignment  
83 constructed using the amino acid sequences of genes shared between the organisms of interest (26).  
84 However, differences in annotation that affect gene calls can add an unnecessary variable when deriving  
85 evolutionary relationships. We propose the use of a nucleotide core genome alignment, constructed  
86 using all collinear genomic regions free of rearrangements (27), to infer phylogenomic relationships.  
87 Using the length of the core genome alignment along with a sequence similarity matrix we aim to assign  
88 taxonomic designations at the genus, species, and strain levels. A core genome alignment-based method  
89 provides advantages to its protein-based counterpart in that it is of a higher resolution, independent of  
90 annotation, transparent with respect to the data used in the calculations, and very amenable to data  
91 sharing and deposition in data repositories.

92 The Rickettsiales are an order within the Alphaproteobacteria is composed of exclusively obligate,  
93 intracellular bacteria where classic DNA-DNA hybridization is not possible and bacterial taxonomy is  
94 uneven, with each of the genera having its own criteria for assigning genus and species designations.

95 Within the Rickettsiales, there are three major families: the Anaplastaceae, Midichloriaceae, and  
96 Rickettsiaceae, with an abundance of genomic data being available for genera within the  
97 Anaplastaceae and Rickettsiaceae. However, species definitions in these families are inconsistent,  
98 and organisms in the *Wolbachia* genus lack community-supported species designations, instead relying  
99 on a system of supergroup designations.

100 The last reorganization of the Rickettsiaceae taxonomy occurred in 2001 (28), a time when there were  
101 <300 sequenced bacterial genomes (29). As of 2014, there have been more than 14,000 genomes  
102 sequenced and with this increase in available genomic information, more informed decisions can be  
103 made with regards to taxonomic classification (29). By using core genome alignments, we can condense  
104 whole genomes into positions shared between the input genomes and use sequence identity to infer  
105 phylogenomic relationships. In this study, we aim to both establish guidelines for delineating bacterial  
106 genus and species boundaries that are consistent with classically-defined genus and species  
107 designations and apply these guidelines to organisms in the Rickettsiales, including *Rickettsia*, *Orientia*,  
108 *Ehrlichia*, *Neohhrlichia*, *Anaplasma*, *Neorickettsia*, and *Wolbachia*.

109 **RESULTS**

110 **Assessment of genus designations**

111 Core genome alignments were generated using the whole genome aligner Mugsy with both complete  
112 and draft genome sequences assembled in  $\leq$ 100 contigs (27). The Mugsy algorithm uses NUCmer to  
113 identify locally colinear blocks (LCBs) between the input genomes, where LCBs are shared colinear  
114 genomic regions free of rearrangements. LCBs found in all organisms are selected and filtered to include  
115 only positions present in all genomes. The resulting core genome alignment is used to generate a  
116 sequence similarity matrix.

117 Core genome alignments were constructed for the *Arcobacter*, *Caulobacter*, *Erwinia*, *Neisseria*,  
118 *Polaribacter*, *Ralstonia*, and *Thermus* genera. Each of the resultant core genome alignments were  $\geq$ 0.33  
119 Mbp in size and represented  $\geq$ 13.6% of the average input genome sizes (**Table 1, Supplementary Table**  
120 **1**), suggesting that the technique is applicable to a wide range of classically defined bacterial taxa.

121 Additionally, core genome alignments were successfully constructed from the genomes of four of the six  
122 Rickettsiales genera, including 69 *Rickettsia* genomes, 3 *Orientia* genomes, 16 *Ehrlichia* genomes, and 23  
123 *Wolbachia* genomes (**Table 1**). Each of these four core genome alignments are  $>$ 0.87 Mbp in length and  
124 contain  $>$ 10% of the average size of the input genomes.

125 We found our initial core genome alignments for *Anaplasma* and *Neorickettsia* to be considerably  
126 shorter, both being  $\sim$ 20 kbp and accounting for  $\leq$ 2.3% of the average input genome sizes. We believe  
127 this reflects that the genomes within these two genera are too broad and need further refinement.  
128 Using input genomes from different genera to construct a core genome alignment yields an alignment of  
129 an insufficient size to accurately represent the evolutionary distances between the input genomes. For  
130 example, when the genome of *Neoehrlichia lotoris* is supplemented to the genomes used to create the  
131 0.49 Mbp *Ehrlichia* core genome alignment, the resultant core genome alignment is 0.11 Mbp,  
132 representing only 8.9% of the average input genome size compared to the prior 39.8%. Therefore, we

133 used subsets of species to test whether the *Anaplasma* and *Neorickettsia* genera are too broadly  
134 defined. A core genome alignment generated using only the 20 *A. phagocytophilum* genomes in the 30  
135 *Anaplasma* genome set is 1.25 Mbp and represents 83.3% of the average input genome size, while a  
136 core genome alignment of the remaining 10 *Anaplasma* genomes is 0.77 Mbp, 65.3% of the average  
137 genome input size. This result suggests that the *Anaplasma* genus should be split into two separate  
138 genera. Similarly, when the genome of *N. helminthoeca* Oregon is excluded from the *Neorickettsia* core  
139 genome alignment, a 0.77 Mbp *Neorickettsia* core genome alignment is generated which represents  
140 87.4% of the average input genome size, suggesting *N. helminthoeca* Oregon is not of the same genus as  
141 the other three *Neorickettsia* genome. For the remainder of the manuscript, these genus  
142 reclassifications are used. Given these collective results we recommend that the genus classification  
143 level can be defined as a group of genomes that together will yield a core genome alignment that  
144 represents  $\geq 10\%$  of the average input genome sizes.

145 **Advantages of nucleotide alignments over protein alignments for bacterial species analyses**

146 While core protein alignments are increasingly used for phylogenetics, a core nucleotide alignment  
147 should have more phylogenetically informative positions in the absence of substitution saturation,  
148 yielding a greater potential for phylogenetic signal. Nucleotide-based analyses outperform amino acid-  
149 based analyses in terms of resolution, branch support, and congruence with independent evidence (30,  
150 31) and outperform amino-acid based analyses at all time scales (32). A core protein alignment  
151 generated from 152 genes shared between the ten complete *Wolbachia* genomes contains 16,241  
152 parsimony-informative positions while the core nucleotide alignment contains 124,074 such positions,  
153 indicating a 10-fold increase in potentially informative positions (**Figure 1**). Substitution saturation can  
154 negatively impact nucleotide-based phylogenetic distance measurements relative to protein-based  
155 phylogenetic methods. However, for each core genome alignment, when the uncorrected pairwise  
156 genetic distances are plotted against the model-corrected distances, linear relationships are observed

157 for all alignments ( $r^2 > 0.995$ ), indicating substitution saturation is not hindering the ability of the core  
158 genome alignments to represent evolutionary relationships (33) (**Supplementary Figure 1**). Given our  
159 results for numerous taxa, we expect this result to be broadly applicable across bacterial species.  
160 Furthermore, maximum likelihood (ML) trees from the core protein alignment and the core nucleotide  
161 alignment are quite similar for branch length as well as topology, except for the wNo branch (**Figure 1**),  
162 which is indicative of a longstanding problem with resolution in the *Wolbachia* phylogeny (34-37).

### 163 **Identifying a CGASI cutoff for species delineation**

164 Within the *Rickettsia*, *Orientia*, *Ehrlichia*, *Anaplasma*, *Neorickettsia*, *Wolbachia*, *Arcobacter*, *Caulobacter*,  
165 *Erwinia*, *Neisseria*, *Polaribacter*, *Ralstonia*, and *Thermus* genome subsets, ANI, dDDH, and CGASI values  
166 were calculated for 7,264 pairwise genome comparisons (**Supplementary Table 2**), of which 601 are  
167 between members of the same species. The ANI and CGASI follow a second-degree polynomial  
168 relationship ( $r^2 = 0.977$ ) (**Figure 2A**). Using this model, the ANI species cutoff of  $\geq 95\%$  is analogous to a  
169 CGASI cutoff of  $\geq 96.8\%$ . The dDDH and CGASI follow a third-degree polynomial model ( $r^2 = 0.978$ ), with a  
170 dDDH of 70% being equivalent to a CGASI of 97.6%, indicating the dDDH species cutoff is generally more  
171 stringent than the ANI species cutoff (**Figure 2B**).

172 The ideal CGASI threshold for species delineation would maximize the prediction of classically defined  
173 species, neither creating nor destroying the majority of the classically defined species. Therefore, all  
174 pairwise comparisons were classified as either intraspecies, between genomes with the same classically  
175 defined species designation, or interspecies, between genomes within the same genus but with  
176 different classically defined species designations. Every possible CGASI threshold value was then tested  
177 for the ability to recapitulate these classically-defined taxonomic classifications (**Figure 2C**). In all cases,  
178 an abnormally high number of interspecies *Rickettsia* comparisons were found above both the  
179 established ANI and dDDH species thresholds consistent with previous observations that guidelines for  
180 establishing novel *Rickettsia* species are too lax (38), and as such they were excluded from this specific

181 analysis. Below a CGASI of 97%, classically defined species begin to be separated while organisms  
182 classically defined as different species begin to be collapsed. This coincides with the above calculated  
183 ANI-equivalent threshold but differs from the above calculated dDDH-equivalent (**Figure 2C**). The dDDH-  
184 equivalent CGASI threshold of 97.6% failed to predict the classically defined taxa from 100 intraspecies  
185 comparisons (**Supplementary Table 3**) while the ANI-equivalent CGASI threshold of 96.8% failed to  
186 predict the classically defined taxa from 41 intraspecies comparisons (**Supplementary Table 4**). Given  
187 these results, we selected the ANI-equivalent CGASI value of  $\geq 96.8\%$  to further analyze these taxa,  
188 which results in our recommendation of specific taxonomic changes within the Rickettsiaceae, including  
189 the *Rickettsia*, *Orientia*, *Anaplasma*, *Ehrlichia*, *Nearickettsia*, and *Wolbachia*.

190 **Rickettsiaceae phylogenomic analyses**

191 ***Rickettsia***

192 The Rickettsiaceae family includes two genera, the *Rickettsia* and the *Orientia*, and while both genera  
193 are obligate intracellular bacteria, *Rickettsia* genomes have undergone more reductive evolution, having  
194 a genome size ranging from 1.1-1.5 Mbp (39) compared to the 2.0-2.2 Mbp size of the *Orientia* genome  
195 (40). Of the Rickettsiales, the *Rickettsia* genus contains the greatest number of sequenced genomes and  
196 named species, containing 69 genome assemblies in  $\leq 100$  contigs representing 27 unique species.  
197 *Rickettsia* genomes are currently classified based on the Fournier criteria, an MLST approach established  
198 in 2003 based on the sequence similarity of five conserved genes: the 16S rRNA, citrate synthase (*gltA*),  
199 and three surface-exposed protein antigens (*ompA*, *ompB*, and gene D) (41). To be considered a  
200 *Rickettsia* species, an isolate must have a sequence similarity of  $\geq 98.1\%$  16S rRNA and  $\geq 86.5\%$  *gltA* to at  
201 least one preexisting *Rickettsia* species. Within the *Rickettsia*, using *ompA*, *ompB*, and gene D sequence  
202 similarities, the Fournier criteria also support the further classification of *Rickettsia* species into three  
203 groups: the typhus group, the spotted fever group (SFG), and the ancestral group (41). However, the

204 Fournier criteria has not yet been amended to classify the more recently established transitional  
205 *Rickettsia* group (42), indicating a need to update the *Rickettsia* taxonomic scheme.  
206 A total of 69 *Rickettsia* genomes representative of 27 different established species were used for ANI,  
207 dDDH, and core genome alignment analyses, and regardless of the method used, a major reclassification  
208 is justified (**Figure 3, Supplementary Table 1**). A core genome alignment constructed using the 69  
209 *Rickettsia* species genomes yielded a core genome alignment size of ~0.56 Mbp, 42.4% of the lengths of  
210 the input *Rickettsia* genomes (**Table 1**). Within the SFG *Rickettsia*, the CGASI between any two genomes  
211 is ≥98.2%, well within the proposed CGASI species cutoff of ≥96.8% (**Figure 3**), while the CGASI is ≤97.2%  
212 in the ancestral and typhus groups. If a CGASI cutoff of 96.8% is used to reclassify the *Rickettsia* species,  
213 all but two of the SFG *Rickettsia* genomes would be classified as the same species (**Figure 3**), with the  
214 two remaining SFG *Rickettsia* genomes, *R. monacensis* IrR Munich and *Rickettsia* sp. Humboldt, being  
215 designated as the same species. This is consistent with ANI as well, while dDDH yields conflicting results  
216 (**Figure 3**). For the transitional group *Rickettsia*, *R. akari* and *R. australis* would be collapsed into a single  
217 species due to having CGASI values of 97.2% with one another. Similarly, *R. asemboensis*, *R. felis*, and  
218 *R. hoogstraalii*, all classified as transitional group *Rickettsia*, would be collapsed into another species, all  
219 having CGASI values of 97.2% with one another. This is consistent with a phylogenomic tree generated  
220 from the *Rickettsia* core genome alignments, where the SFG *Rickettsia* genomes have far less sequence  
221 divergence compared to the rest of the *Rickettsia* genomes (**Figure 3**).

222 ***Orientia***  
223 The organisms within *Orientia* have no standardized criteria to define novel species, with *Orientia chuto*  
224 being defined as a novel species based on geographical location and the phylogenetic clustering of the  
225 16S rRNA and two protein coding genes that encode for serine protease *htrA* (47 kDa gene) and an outer  
226 membrane protein (56-kDa gene), respectively (43). There are far fewer high-quality *Orientia* genomes,  
227 which is partly due to the large number of repeat elements found in *Orientia* genomes, with the genome

228 of *Orientia tsutsugamushi* being the most highly repetitive sequenced bacterial genome to date with  
229 ~42% of its genome being comprised of short repetitive sequences and transposable elements (44).  
230 The *Orientia* core genome alignment was constructed using three *O.tsutsugamushi* genomes and is 0.97  
231 Mbp in size, ~47.6% of the average input genome size, with CGASI values ranging from 96.3-97.2%  
232 (**Supplementary Figure 2**). Reclassifying the *Orientia* genomes using a CGASI species cutoff of 96.8%  
233 would result in *O. tsutsugamushi* Gilliam and *O.tsutsugamushi* Ikeda being classified as a separate  
234 species from *O. tsutsugamushi* Boryong (**Supplementary Figure 2**). In this case, this reclassification  
235 would not be consistent with recommendations from using ANI or dDDH, which is likely in part due to an  
236 imperfect correlation with the ANI and dDDH species cutoffs (18). In this case, we suspect that ANI is  
237 strongly influenced by the large number of repeats in the genome due to ANI calculations being based  
238 off the sequence identity of 1 kbp query genome fragments. In comparison, we do not anticipate that  
239 whole genome alignments would be confounded by the repeats. While the LCBs may be fragmented by  
240 the repeats, creating smaller syntenic blocks, the non-phylogenetically informative repeats are  
241 eliminated from an LCB-based analysis.

## 242 **Anaplasmataceae phylogenomic analyses**

### 243 ***Ehrlichia***

244 Within the Anaplasmataceae, species designations are frequently assigned based on sequence similarity  
245 and clustering patterns from phylogenetic analyses generated using the sequences of specific genes, like  
246 the 16S rRNA, *groEL*, and *gltA* (45). As an example, the species designations for *Ehrlichia khabarensis*  
247 and *Ehrlichia ornithorhynchi* are justified based on having a lower sequence similarity for the 16S rRNA,  
248 *groEL*, and *gltA* below the maximum similarity that differentiates other *Ehrlichia* species (45-47).

249 A core genome alignment constructed using 16 *Ehrlichia* genomes, representative of four defined  
250 species, yields a 0.49 Mbp alignment, which equates to 39.8% of the average *Ehrlichia* genome size (1.25  
251 Mbp) (**Table 1**). Using a CGASI species cutoff of 96.8%, the *Ehrlichia chaffeensis* and *Ehrlichia ruminantium*

252 genomes were recovered as monophyletic and well supported species, which is consistent with dDDH  
253 and ANI (**Figure 4**). The two *Ehrlichia muris* and *Ehrlichia* sp. Wisconsin\_h genomes have CGASI values  
254 >97.8%, indicating the three genomes represent one species, which is consistent with ANI, but not dDDH  
255 (**Figure 4**). The genomes of *Ehrlichia* sp. HF and *E. canis* Jake do not have CGASI values  $\geq$ 96.8% with any  
256 other species, confirming their status as individual species, consistent with dDDH and ANI (**Figure 4**).  
257 This is consistent with an *Ehrlichia* phylogenomic tree (**Figure 4**).

258 ***Anaplasma***

259 A novel *Anaplasma* species is currently defined based on phylogenetic analyses involving the 16S rRNA,  
260 *gltA*, and *groEL*, with a new species having a lower sequence identity and a divergent phylogenetic  
261 position relative to established *Anaplasma* species (48-51). A core genome alignment constructed using  
262 30 *Anaplasma* genomes yielded a 20 kbp alignment, 1.4% of the average input genome size. As noted  
263 before, such low values are indicative of more than one genus represented in the taxa included in the  
264 analysis. Thus, CGASI analyses for the *Anaplasma* were done on two *Anaplasma* genome subsets, one  
265 containing the twenty *Anaplasma phagocytophilum* genomes and the other containing nine *Anaplasma*  
266 *marginale* and one *Anaplasma centrale* genomes (**Table 1**).

267 A 1.25 Mbp core genome alignment, consisting of 39.8% of the average input genome size, was  
268 constructed using twenty *A. phagocytophilum* genomes that all have CGASI values of  $\geq$ 96.8%, supporting  
269 their designation as members of a single species (**Figure 5**). This is supported by ANI, but dDDH again  
270 yields conflicting results (**Figure 5**). The core genome alignment generated using the remaining ten  
271 *Anaplasma* genomes yields a 0.77 Mbp core genome alignment, 65.3% of the average input genome  
272 size. The *A. centrale* genome has CGASI values ranging from 90.7-91.0% when compared to the nine *A.*  
273 *marginale* genomes, supporting *A. centrale* as a separate species from *A. marginale*, consistent with  
274 existing taxonomy and with the ANI and dDDH species cutoffs (**Figure 5**).

275 ***Neorickettsia***

276 The *Neorickettsia* genus contains four genome assemblies: *Neorickettsia helminthoeca* Oregon,  
277 *Neorickettsia risticii* Illinois, *Neorickettsia sennetsu* Miyayama, and *Neorickettsia* sp. 179522. The genus  
278 was first established in 1954 with the discovery of *N. helminthoeca* (52) and in 2001, *N. risticii* and *N*  
279 *sennetsu*, both initially classified as *Ehrlichia* strains, were added to the *Neorickettsia* based on  
280 phylogenetic analyses of 16S rRNA and *groESL* (28). A core genome alignment constructed using all four  
281 *Neorickettsia* genomes yields a 20 kbp alignment, 2.3% of the average input genome size. When  
282 excluding the genome of *N. helminthoeca* Oregon, the three remaining *Neorickettsia* genomes form a  
283 core genome alignment of 0.76 Mbp in size, 87.4% of the average input genome size, indicating *N. risticii*  
284 Illinois, *N. sennetsu* Miyayama, and *Neorickettsia* sp. 179522 are three distinct species within the same  
285 genus while *N. helminthoeca* Oregon is of a separate genus (**Supplementary Figure 3**). When assessing  
286 the *Neorickettsia* species designations using ANI and dDDH cutoffs, the four *Neorickettsia* genomes can  
287 only be determined to be different species, as the two techniques are unable to delineate phylogenomic  
288 relationships at the genus level.

289 ***Wolbachia***  
290 The current *Wolbachia* classification system currently lacks traditional species designations and instead  
291 groups organisms by supergroup designations using an MLST system consisting of 450-500 bp internal  
292 fragments of five genes, *gatB*, *coxA*, *hcpA*, *ftsZ*, and *fbpA* (53). A core genome alignment generated using  
293 23 *Wolbachia* genomes yields a 0.18 Mbp alignment, amounting to 14.8% of the average input genome  
294 size. The CGASI values between the supergroup A *Wolbachia*, apart from *wlnc* SM, have CGASI values  
295  $\geq 96.8$  (**Figure 6**). The genome of *wlnc* SM has CGASI values ranging from 94.6%-95.9% when compared  
296 to other supergroup A *Wolbachia*, indicating that *wlnc* SM is a different species. This is also supported  
297 by ANI and, with a few exceptions, dDDH. However, a phylogenomic tree generated using the *Wolbachia*  
298 core genome alignment indicates *wlnc* SM is nested within the other supergroup A *Wolbachia* taxa, a  
299 clade with 100% bootstrap support (**Figure 6**). The ANI, dDDH, and CGASI values of *wlnc* SM are likely

300 underestimated due to >10% of the genome having ambiguous nucleotide positions, leading to large  
301 penalties in sequence identity scores, indicating that these methods may not be suited for genomes with  
302 large numbers of ambiguous positions. Among the filarial *Wolbachia* supergroups C and D, the CGASI  
303 cutoff of 96.8% would split each of the traditionally recognized supergroups into two groups each, also  
304 supported by ANI and dDDH. While *wOo* and *wOv* would be the same species, *wDi* Pavia should be  
305 considered a different species. Similarly, *wBm* and *wWb* would be considered the same species, while  
306 *wLs* should be designated as a separate species. The *wCle*, *wFol*, and *wPpe* endosymbionts from  
307 supergroups E, F, and L, respectively, would all be considered distinct species using CGASI, ANI, or dDDH.  
308 The results between CGASI, ANI, and dDDH in supergroup B are discordant. Five of the six supergroup B  
309 *Wolbachia* genomes, all except for *wTpre*, have CGASI values  $\geq$ 96.8% when compared to one of the  
310 other five, indicating the five genomes are of the same species. However, despite *wTpre* being  
311 considered a different species if the CGASI cutoff of 96.8% is used, a phylogenomic tree constructed  
312 using the core genome alignment shows *wTpre* to be nested within the supergroup B *Wolbachia* (**Figure**  
313 **6**). If *wTpre* is designated as a different species, this would create a paraphyletic clade in the supergroup  
314 B *Wolbachia*, suggesting that *wTpre* is not a different species, but rather should be included with the  
315 other supergroup B *Wolbachia* as a single species. When assessing the ANI and dDDH values between  
316 the supergroup B *Wolbachia*, only *wPip* JHB and *wPip* Pel share both ANI values  $\geq$ 95% and dDDH values  
317  $\geq$ 70% with one another (**Figure 6**). The remaining three supergroup B *Wolbachia*, *wNo*, *wStri*, and *wAus*  
318 have ANI values  $\geq$ 95% with some of the other supergroup B *Wolbachia* while not having a dDDH  $\geq$ 70%  
319 with any other genome, suggesting each supergroup B genome may be a separate species. Currently,  
320 the underlying basis for the differences in CGASI, ANI, and dDDH in supergroup B *Wolbachia*  
321 endosymbionts are not apparent. Given tradition, we would recommend caution and label all  
322 supergroup B *Wolbachia* as a single species with a potential re-evaluation in the future.  
323 **Other taxa**

324 Overall, there were 41 pairwise comparisons of organisms across diverse taxa including *Arcobacter*,  
325 *Caulobacter*, *Neisseria*, *Orientia*, *Ralstonia*, and *Thermus* that are classically defined as the same species  
326 but would be classified as distinct species when assessed using our suggested CGASI threshold  
327 (**Supplementary Table 4**). Additionally, there were 782 pairwise comparisons of organisms classically  
328 defined as different species that this threshold suggests should be the same species, of which only 10  
329 were not in the genus *Rickettsia*, instead belonging to the *Arcobacter* and *Caulobacter* (**Supplementary**  
330 **Table 5**). This suggests that using CGASI with this threshold yields robust results. However, as seen with  
331 the supergroup B *Wolbachia* results, using strictly a nucleotide identity-based threshold can lead to  
332 paraphyletic groups, such that examination with a phylogenomic tree constructed using the core  
333 genome alignment is recommended, as was also observed for *Neisseria*.

334 A 0.33 Mbp core genome alignment was generated from 66 *Neisseria* genomes, accounting for 14.7% of  
335 the average input genome size. The core genome alignment largely supports the classically defined  
336 species including *N. meningitidis*, *N. gonorrhoeae*, *N. weaveri*, and *N. lactamica*, although one *N.*  
337 *lactamica* isolate, *N. lactamica* 338.rep1\_NLAC, appears to be inaccurately assigned (**Supplementary**  
338 **Figure 4**). The CGASI values suggest each *N. elongata* isolate is a distinct species, as are the *N. flavescens*  
339 isolates. Like what was observed in the *Wolbachia*, a paraphyletic clade is observed when using a CGASI  
340 cutoff of 98.6% with the genome of *Neisseria* sp. HMSC061B04 being nested within a clade of two *N.*  
341 *mucosa* genomes, *N. lactamica* 338.rep1\_NLAC, and several unnamed *Neisseria* taxa, while not having a  
342 CGASI  $\geq$ 98.6% when compared to any other *Neisseria* genome (**Supplementary Figure 4**). This highlights  
343 that while sequence identity cutoffs derived using nucleotide-based pairwise comparisons are important  
344 when delineating species, analyses using phylogenomic trees can aid in resolving instances near the  
345 CGASI species cutoff to ensure that paraphyletic clades do not occur. The two results are quite  
346 complimentary with the core genome alignment being amenable to ML-based phylogenetic approaches.

347 **DISCUSSION**

348 As noted with the development of MLST (54), sequence data has the advantages of being incredibly  
349 standardized and portable. While MLST methods allow for insight at the sub-species levels of taxonomic  
350 classifications, and are heavily relied upon during infectious disease outbreaks, they do not provide  
351 sufficient resolution at the species level. Increased resolution is required when inferring evolutionary  
352 relationships and can be obtained through the construction of whole genome alignments that maximize  
353 the number of evolutionarily informative positions.

354 By generating core genome alignments for different genera, we sought to identify a universal, high-  
355 resolution method for species classification. Using the core genome alignment, a set of genomes can be  
356 analyzed based on both the length and sequence identity of its core genome alignment. The length of  
357 the core genome alignment, which reflects the ability for the genomes to be aligned, is informative in  
358 delineating genera. Meanwhile, the pairwise comparisons of core genome alignment sequence identity  
359 can be used to delineate species, which can in turn be further validated with a phylogenetic analysis that  
360 can be used to resolve paraphyletic clades.

361 A current issue of the Mugsy aligner is the inability for the software to scale, being only able to  
362 computationally handle subsets of at most ~80 genomes. However, for heavily sequenced genera such  
363 as the *Rickettsia*, future species assignments for novel genomes do not require constructing a core  
364 genome alignment from every available genome to infer evolutionary relationships. Instead, we  
365 recommend that for each genus, the relevant experts in the community establish and curate a set of  
366 trusted genomes with at least one representative of each named species that should be used for  
367 constructing core genome alignments. After an initial assessment, refinement could then be made using  
368 a core genome alignment with many more genomes from closely related species.

369 Through this work we have identified criteria that largely reconstruct classical species definitions in a  
370 method that is transparent and portable. In the course of this work we have identified modifications

371 that need to be made to the species and genus designations of a number of organisms, particularly  
372 within the Rickettsiales. While we have identified these instances, we recommend that any changes in  
373 nomenclature be addressed by collaborative teams of experts in the respective communities.

## 374 **MATERIALS AND METHODS**

### 375 **Core genome alignments**

376 Genomes used in the taxonomic analyses were downloaded from NCBI GenBank (55). OrthoANIu v1.2  
377 (56) and USEARCH v6.1.544 (57) were used for the average nucleotide identity calculations. GGDC v2.1  
378 (ggdc.dsmz.de) (25) paired with the recommended BLAST+ alignment tool (58) was used to calculate  
379 dDDH values. For analyses in this paper, all dDDH calculations were performed using dDDH formula 2  
380 due to the usage of draft genomes in taxonomic analyses (24). Core genome alignments were generated  
381 for each of the genome subsets using Mugsy v1.2 (27) and MOTHUR v1.22 (59). Sequence identity  
382 matrices for the core genome alignments were created using BioEdit v7.2.5  
383 (brownlab.mbio.ncsu.edu/JWB/papers/1999Hall1.pdf). ML phylogenomic trees with 1000 bootstraps  
384 were calculated for each core genome alignment using IQ-TREE v1.6.2 (60) paired with ModelFinder (61)  
385 to select the best model of evolution and UFBoot2 (62) for fast bootstrap approximation. Trees were  
386 visualized and annotated using iTOL v4.1.1 (63). Construction of neighbor-network trees were done  
387 using the R packages ape (64) and phangorn (65).

### 388 **Core protein alignments**

389 Orthologs between complete genomes of the same species were determined using FastOrtho, a  
390 reimplementation of OrthoMCL (66) that identifies orthologs using all by all BLAST searches. The amino  
391 acid sequences of proteins present in all organisms in only one copy were aligned using MAAFT v7.313  
392 (67). For every protein alignment, the best model of evolution was identified using ModelFinder (61) and  
393 phylogenomic trees were constructed using an edge-proportional partition model (68) with IQ-TREE

394 v1.6.2 (60) and UFBoot2 (62) for fast bootstrap approximation. Comparative analyses of core protein  
395 and core nucleotide alignment trees were done using the R packages ape (64) and phangorn (65).

396 **ACKNOWLEDGMENTS**

397 We would like to thank Dr. Joseph J. Gillespie for helpful discussions and encouragement. This work was  
398 funded by the National Institute of Allergy and Infectious Diseases (U19AI110820).

399 **REFERENCES**

400 1. Gould SJ, William B. Provine Collection on Evolution and Genetics. 1984. Hen's teeth and  
401 horse's toes. Norton, New York.

402 2. Ramasamy D, Mishra AK, Lagier JC, Padhmanabhan R, Rossi M, Sentausa E, Raoult D,  
403 Fournier PE. 2014. A polyphasic strategy incorporating genomic data for the taxonomic  
404 description of novel bacterial species. *Int J Syst Evol Microbiol* 64:384-91.

405 3. Schleifer KH. 2009. Classification of Bacteria and Archaea: past, present and future. *Syst  
406 Appl Microbiol* 32:533-42.

407 4. Bisen PS, Debnath M, Prasad GB. 2012. Identification and Classification of Microbes. *In  
408 P. S. Bisen MDaGBP (ed), Microbes* doi:doi:10.1002/9781118311912.ch4.

409 5. Rossello-Mora R, Amann R. 2001. The species concept for prokaryotes. *FEMS Microbiol  
410 Rev* 25:39-67.

411 6. Brenner DJ, Fanning GR, Steigerwalt AG. 1972. Deoxyribonucleic acid relatedness among  
412 species of *Erwinia* and between *Erwinia* species and other enterobacteria. *J Bacteriol*  
413 110:12-7.

414 7. Dubnau D, Smith I, Morell P, Marmur J. 1965. Gene conservation in *Bacillus* species. I.  
415 Conserved genetic and nucleic acid base sequence homologies. *Proc Natl Acad Sci U S A*  
416 54:491-8.

417 8. Boone DR, Castenholz RW, SpringerLink (Online service). 2001. *Bergey's Manual® of  
418 Systematic Bacteriology : Overview: A Phylogenetic Backbone and Taxonomic  
419 Framework for Prokaryotic Systematics*, Second Edition. ed. Springer New York : Imprint:  
420 Springer, New York, NY.

421 9. Quast C, Pruesse E, Yilmaz P, Gerken J, Schweer T, Yarza P, Peplies J, Glockner FO. 2013.  
422 The SILVA ribosomal RNA gene database project: improved data processing and web-  
423 based tools. *Nucleic Acids Res* 41:D590-6.

424 10. McDonald D, Price MN, Goodrich J, Nawrocki EP, DeSantis TZ, Probst A, Andersen GL,  
425 Knight R, Hugenholtz P. 2012. An improved Greengenes taxonomy with explicit ranks for  
426 ecological and evolutionary analyses of bacteria and archaea. *ISME J* 6:610-8.

427 11. Palys T, Nakamura LK, Cohan FM. 1997. Discovery and classification of ecological  
428 diversity in the bacterial world: the role of DNA sequence data. *Int J Syst Bacteriol*  
429 47:1145-56.

430 12. Janda JM, Abbott SL. 2007. 16S rRNA gene sequencing for bacterial identification in the  
431 diagnostic laboratory: pluses, perils, and pitfalls. *J Clin Microbiol* 45:2761-4.

432 13. Rossello-Mora R, Amann R. 2015. Past and future species definitions for Bacteria and  
433 Archaea. *Syst Appl Microbiol* 38:209-16.

434 14. Yarza P, Yilmaz P, Pruesse E, Glockner FO, Ludwig W, Schleifer KH, Whitman WB, Euzeby  
435 J, Amann R, Rossello-Mora R. 2014. Uniting the classification of cultured and uncultured  
436 bacteria and archaea using 16S rRNA gene sequences. *Nat Rev Microbiol* 12:635-45.

437 15. Chun J, Oren A, Ventosa A, Christensen H, Arahal DR, da Costa MS, Rooney AP, Yi H, Xu  
438 XW, De Meyer S, Trujillo ME. 2018. Proposed minimal standards for the use of genome  
439 data for the taxonomy of prokaryotes. *Int J Syst Evol Microbiol* 68:461-466.

440 16. Karlsson R, Gonzales-Siles L, Boulund F, Svensson-Stadler L, Skovbjerg S, Karlsson A,  
441 Davidson M, Hulth S, Kristiansson E, Moore ER. 2015. Proteotyping: Proteomic

442 characterization, classification and identification of microorganisms--A prospectus. *Syst Appl Microbiol* 38:246-57.

444 17. De Bruyne K, Slabbinck B, Waegeman W, Vauterin P, De Baets B, Vandamme P. 2011.

445 Bacterial species identification from MALDI-TOF mass spectra through data analysis and

446 machine learning. *Syst Appl Microbiol* 34:20-9.

447 18. Goris J, Konstantinidis KT, Klappenbach JA, Coenye T, Vandamme P, Tiedje JM. 2007.

448 DNA-DNA hybridization values and their relationship to whole-genome sequence

449 similarities. *Int J Syst Evol Microbiol* 57:81-91.

450 19. Gevers D, Cohan FM, Lawrence JG, Spratt BG, Coenye T, Feil EJ, Stackebrandt E, Van de

451 Peer Y, Vandamme P, Thompson FL, Swings J. 2005. Opinion: Re-evaluating prokaryotic

452 species. *Nat Rev Microbiol* 3:733-9.

453 20. Auch AF, von Jan M, Klenk HP, Goker M. 2010. Digital DNA-DNA hybridization for

454 microbial species delineation by means of genome-to-genome sequence comparison.

455 *Stand Genomic Sci* 2:117-34.

456 21. Aanensen DM, Spratt BG. 2005. The multilocus sequence typing network: *mlst.net*.

457 *Nucleic Acids Res* 33:W728-33.

458 22. Larsen MV, Cosentino S, Rasmussen S, Friis C, Hasman H, Marvig RL, Jelsbak L, Sicheritz-

459 Ponten T, Ussery DW, Aarestrup FM, Lund O. 2012. Multilocus sequence typing of total-

460 genome-sequenced bacteria. *J Clin Microbiol* 50:1355-61.

461 23. Kurtz S, Phillippy A, Delcher AL, Smoot M, Shumway M, Antonescu C, Salzberg SL. 2004.

462 Versatile and open software for comparing large genomes. *Genome Biol* 5:R12.

463 24. Auch AF, Klenk HP, Goker M. 2010. Standard operating procedure for calculating  
464 genome-to-genome distances based on high-scoring segment pairs. *Stand Genomic Sci*  
465 2:142-8.

466 25. Meier-Kolthoff JP, Auch AF, Klenk HP, Goker M. 2013. Genome sequence-based species  
467 delimitation with confidence intervals and improved distance functions. *BMC*  
468 *Bioinformatics* 14:60.

469 26. Tettelin H, Maignani V, Cieslewicz MJ, Donati C, Medini D, Ward NL, Angiuoli SV,  
470 Crabtree J, Jones AL, Durkin AS, Deboy RT, Davidsen TM, Mora M, Scarselli M, Margarit y  
471 Ros I, Peterson JD, Hauser CR, Sundaram JP, Nelson WC, Madupu R, Brinkac LM, Dodson  
472 RJ, Rosovitz MJ, Sullivan SA, Daugherty SC, Haft DH, Selengut J, Gwinn ML, Zhou L, Zafar  
473 N, Khouri H, Radune D, Dimitrov G, Watkins K, O'Connor KJ, Smith S, Utterback TR,  
474 White O, Rubens CE, Grandi G, Madoff LC, Kasper DL, Telford JL, Wessels MR, Rappuoli  
475 R, Fraser CM. 2005. Genome analysis of multiple pathogenic isolates of *Streptococcus*  
476 *agalactiae*: implications for the microbial "pan-genome". *Proc Natl Acad Sci U S A*  
477 102:13950-5.

478 27. Angiuoli SV, Salzberg SL. 2011. Mugsy: fast multiple alignment of closely related whole  
479 genomes. *Bioinformatics* 27:334-42.

480 28. Dumler JS, Barbet AF, Bekker CP, Dasch GA, Palmer GH, Ray SC, Rikihisa Y, Rurangirwa  
481 FR. 2001. Reorganization of genera in the families Rickettsiaceae and Anaplasmataceae  
482 in the order Rickettsiales: unification of some species of *Ehrlichia* with *Anaplasma*,  
483 *Cowdria* with *Ehrlichia* and *Ehrlichia* with *Neorickettsia*, descriptions of six new species

484 combinations and designation of *Ehrlichia equi* and 'HGE agent' as subjective synonyms  
485 of *Ehrlichia phagocytophila*. *Int J Syst Evol Microbiol* 51:2145-65.

486 29. Land M, Hauser L, Jun SR, Nookaew I, Leuze MR, Ahn TH, Karpinets T, Lund O, Kora G,  
487 Wassenaar T, Poudel S, Ussery DW. 2015. Insights from 20 years of bacterial genome  
488 sequencing. *Funct Integr Genomics* 15:141-61.

489 30. Simmons MP, Ochoterena H, Freudenstein JV. 2002. Amino acid vs. nucleotide  
490 characters: challenging preconceived notions. *Mol Phylogenet Evol* 24:78-90.

491 31. Simmons MP, Carr TG, O'Neill K. 2004. Relative character-state space, amount of  
492 potential phylogenetic information, and heterogeneity of nucleotide and amino acid  
493 characters. *Mol Phylogenet Evol* 32:913-26.

494 32. Townsend JP, Lopez-Giraldez F, Friedman R. 2008. The phylogenetic informativeness of  
495 nucleotide and amino acid sequences for reconstructing the vertebrate tree. *J Mol Evol*  
496 67:437-47.

497 33. Philippe H, Forterre P. 1999. The rooting of the universal tree of life is not reliable. *J Mol*  
498 *Evol* 49:509-23.

499 34. Bordenstein SR, Paraskevopoulos C, Dunning Hotopp JC, Sapountzis P, Lo N, Bandi C,  
500 Tettelin H, Werren JH, Bourtzis K. 2009. Parasitism and mutualism in *Wolbachia*: what  
501 the phylogenomic trees can and cannot say. *Mol Biol Evol* 26:231-241.

502 35. Casiraghi M, Bordenstein SR, Baldo L, Lo N, Beninati T, Wernegreen JJ, Werren JH, Bandi  
503 C. 2005. Phylogeny of *Wolbachia pipiensis* based on *gltA*, *groEL* and *ftsZ* gene  
504 sequences: clustering of arthropod and nematode symbionts in the F supergroup, and  
505 evidence for further diversity in the *Wolbachia* tree. *Microbiology* 151:4015-22.

506 36. Lefoulon E, Bain O, Makepeace BL, d'Haese C, Uni S, Martin C, Gavotte L. 2016.  
507 Breakdown of coevolution between symbiotic bacteria Wolbachia and their filarial  
508 hosts. *PeerJ* 4:e1840.

509 37. Gerth M, Gansauge MT, Weigert A, Bleidorn C. 2014. Phylogenomic analyses uncover  
510 origin and spread of the Wolbachia pandemic. *Nat Commun* 5:5117.

511 38. Walker DH, Ismail N. 2008. Emerging and re-emerging rickettsioses: endothelial cell  
512 infection and early disease events. *Nat Rev Microbiol* 6:375-86.

513 39. Georgiades K, Merhej V, El Karkouri K, Raoult D, Pontarotti P. 2011. Gene gain and loss  
514 events in *Rickettsia* and *Orientia* species. *Biol Direct* 6:6.

515 40. Liao HM, Chao CC, Lei H, Li B, Tsai S, Hung GC, Ching WM, Lo SC. 2017. Intraspecies  
516 comparative genomics of three strains of *Orientia tsutsugamushi* with different  
517 antibiotic sensitivity. *Genom Data* 12:84-88.

518 41. Fournier PE, Dumler JS, Greub G, Zhang J, Wu Y, Raoult D. 2003. Gene sequence-based  
519 criteria for identification of new rickettsia isolates and description of *Rickettsia*  
520 *heilongjiangensis* sp. nov. *J Clin Microbiol* 41:5456-65.

521 42. Gillespie JJ, Beier MS, Rahman MS, Ammerman NC, Shallom JM, Purkayastha A, Sobral  
522 BS, Azad AF. 2007. Plasmids and rickettsial evolution: insight from *Rickettsia felis*. *PLoS*  
523 *One* 2:e266.

524 43. Izzard L, Fuller A, Blacksell SD, Paris DH, Richards AL, Aukkanit N, Nguyen C, Jiang J,  
525 Fenwick S, Day NP, Graves S, Stenos J. 2010. Isolation of a novel *Orientia* species (*O.*  
526 *chuto* sp. nov.) from a patient infected in Dubai. *J Clin Microbiol* 48:4404-9.

527 44. Salje J. 2017. *Orientia tsutsugamushi*: A neglected but fascinating obligate intracellular  
528 bacterial pathogen. *PLoS Pathog* 13:e1006657.

529 45. Rar VA, Pukhovskaya NM, Ryabchikova EI, Vysochina NP, Bakhmetyeva SV, Zdanovskaia  
530 NI, Ivanov LI, Tikunova NV. 2015. Molecular-genetic and ultrastructural characteristics of  
531 'Candidatus Ehrlichia khabarensis', a new member of the Ehrlichia genus. *Ticks Tick*  
532 *Borne Dis* 6:658-67.

533 46. Inokuma H, Brouqui P, Drancourt M, Raoult D. 2001. Citrate synthase gene sequence: a  
534 new tool for phylogenetic analysis and identification of Ehrlichia. *J Clin Microbiol*  
535 39:3031-9.

536 47. Gofton AW, Loh SM, Barbosa AD, Paparini A, Gillett A, Macgregor J, Oskam CL, Ryan UM,  
537 Irwin PJ. 2018. A novel Ehrlichia species in blood and *Ixodes ornithorhynchi* ticks from  
538 platypuses (*Ornithorhynchus anatinus*) in Queensland and Tasmania, Australia. *Ticks*  
539 *Tick Borne Dis* 9:435-442.

540 48. Ybanez AP, Matsumoto K, Kishimoto T, Inokuma H. 2012. Molecular analyses of a  
541 potentially novel *Anaplasma* species closely related to *Anaplasma phagocytophilum*  
542 detected in sika deer (*Cervus nippon yesoensis*) in Japan. *Vet Microbiol* 157:232-6.

543 49. Li H, Zheng YC, Ma L, Jia N, Jiang BG, Jiang RR, Huo QB, Wang YW, Liu HB, Chu YL, Song  
544 YD, Yao NN, Sun T, Zeng FY, Dumler JS, Jiang JF, Cao WC. 2015. Human infection with a  
545 novel tick-borne *Anaplasma* species in China: a surveillance study. *Lancet Infect Dis*  
546 15:663-70.

547 50. Yang J, Liu Z, Niu Q, Liu J, Han R, Liu G, Shi Y, Luo J, Yin H. 2016. Molecular survey and  
548 characterization of a novel *Anaplasma* species closely related to *Anaplasma capra* in  
549 ticks, northwestern China. *Parasit Vectors* 9:603.

550 51. Battilani M, De Arcangeli S, Balboni A, Dondi F. 2017. Genetic diversity and molecular  
551 epidemiology of *Anaplasma*. *Infect Genet Evol* 49:195-211.

552 52. Philip CB, Hadlow WJ, Hughes LE. 1954. Studies on salmon poisoning disease of canines.  
553 I. The rickettsial relationships and pathogenicity of *Neorickettsia helmintheca*. *Exp  
554 Parasitol* 3:336-50.

555 53. Baldo L, Dunning Hotopp JC, Jolley KA, Bordenstein SR, Biber SA, Choudhury RR, Hayashi  
556 C, Maiden MC, Tettelin H, Werren JH. 2006. Multilocus sequence typing system for the  
557 endosymbiont *Wolbachia pipiensis*. *Appl Environ Microbiol* 72:7098-110.

558 54. Maiden MC, Bygraves JA, Feil E, Morelli G, Russell JE, Urwin R, Zhang Q, Zhou J, Zurth K,  
559 Caugant DA, Feavers IM, Achtman M, Spratt BG. 1998. Multilocus sequence typing: a  
560 portable approach to the identification of clones within populations of pathogenic  
561 microorganisms. *Proc Natl Acad Sci U S A* 95:3140-5.

562 55. Benson DA, Cavanaugh M, Clark K, Karsch-Mizrachi I, Lipman DJ, Ostell J, Sayers EW.  
563 2013. GenBank. *Nucleic Acids Res* 41:D36-42.

564 56. Yoon SH, Ha SM, Lim J, Kwon S, Chun J. 2017. A large-scale evaluation of algorithms to  
565 calculate average nucleotide identity. *Antonie Van Leeuwenhoek* 110:1281-1286.

566 57. Edgar RC. 2010. Search and clustering orders of magnitude faster than BLAST.  
567 *Bioinformatics* 26:2460-1.

568 58. Camacho C, Coulouris G, Avagyan V, Ma N, Papadopoulos J, Bealer K, Madden TL. 2009.

569 BLAST+: architecture and applications. *BMC Bioinformatics* 10:421.

570 59. Schloss PD, Westcott SL, Ryabin T, Hall JR, Hartmann M, Hollister EB, Lesniewski RA,

571 Oakley BB, Parks DH, Robinson CJ, Sahl JW, Stres B, Thallinger GG, Van Horn DJ, Weber

572 CF. 2009. Introducing mothur: open-source, platform-independent, community-

573 supported software for describing and comparing microbial communities. *Appl Environ*

574 *Microbiol* 75:7537-41.

575 60. Nguyen LT, Schmidt HA, von Haeseler A, Minh BQ. 2015. IQ-TREE: a fast and effective

576 stochastic algorithm for estimating maximum-likelihood phylogenies. *Mol Biol Evol*

577 32:268-74.

578 61. Kalyaanamoorthy S, Minh BQ, Wong TKF, von Haeseler A, Jermiin LS. 2017.

579 ModelFinder: fast model selection for accurate phylogenetic estimates. *Nat Methods*

580 14:587-589.

581 62. Hoang DT, Chernomor O, von Haeseler A, Minh BQ, Vinh LS. 2018. UFBoot2: Improving

582 the Ultrafast Bootstrap Approximation. *Mol Biol Evol* 35:518-522.

583 63. Letunic I, Bork P. 2016. Interactive tree of life (iTOL) v3: an online tool for the display

584 and annotation of phylogenetic and other trees. *Nucleic Acids Res* 44:W242-5.

585 64. Paradis E, Claude J, Strimmer K. 2004. APE: Analyses of Phylogenetics and Evolution in R

586 language. *Bioinformatics* 20:289-90.

587 65. Schliep KP. 2011. phangorn: phylogenetic analysis in R. *Bioinformatics* 27:592-3.

588 66. Li L, Stoeckert CJ, Jr., Roos DS. 2003. OrthoMCL: identification of ortholog groups for

589 eukaryotic genomes. *Genome Res* 13:2178-89.

590 67. Katoh K, Misawa K, Kuma K, Miyata T. 2002. MAFFT: a novel method for rapid multiple  
591 sequence alignment based on fast Fourier transform. *Nucleic Acids Res* 30:3059-66.

592 68. Chernomor O, von Haeseler A, Minh BQ. 2016. Terrace Aware Data Structure for  
593 Phylogenomic Inference from Supermatrices. *Syst Biol* 65:997-1008.

594

595 **FIGURE LEGENDS**

596 **Figure 1: Comparison of phylogenomic trees generated using the core nucleotide and core**  
597 **protein alignments for ten complete *Wolbachia* genomes**

598 Two phylogenomic trees were generated from the genomes of ten *Wolbachia* strains using **(A)** a core  
599 protein alignment (CPA) containing 152 genes present in only one copy in all ten genomes and **(B)** a core  
600 genome alignment (CNA) with members of the *Wolbachia* supergroups A (●), B (▲), C (■), D (◆), and F  
601 (●) being represented. Shapes of the same color indicate that the multiple genomes are of the same  
602 species as determined using our determined CGASI cutoff of  $\geq 96.8\%$ . The single difference in topology is  
603 denoted in grey, otherwise the trees are largely similar in both topology and branch lengths, despite the  
604 core protein alignment being 77,868 bp long with 16,241 parsimony-informative positions while the  
605 core nucleotide alignment is 579,495 bp long with 124,074 such positions.

606 **Figure 2: ANI, dDDH, and CGASI correlation analysis**

607 CGASI, ANI and dDDH values were calculated for 7,264 pairwise comparisons of genomes within the  
608 same genus for *Rickettsia*, *Orientia*, *Ehrlichia*, *Anaplasma*, *Neorickettsia*, *Wolbachia*, *Caulobacter*,  
609 *Erwinia*, *Neisseria*, *Polaribacter*, *Ralstonia*, and *Thermus*. **(A)** The CGASI and ANI values for the  
610 interspecies comparisons follow a second-degree polynomial model ( $r^2 = 0.977$ ) with the ANI species  
611 cutoff of  $\geq 95\%$  being equivalent to a CGASI of 96.8%, indicated by the blue dotted box. **(B)** The CGASI  
612 and dDDH values for all pairwise comparisons follow a third-degree polynomial model ( $r^2 = 0.978$ ) with  
613 the dDDH species cutoff of  $\geq 70\%$  being equivalent to a CGASI of 97.6%, indicated by the red dotted box.  
614 **(C)** To identify the optimal CGASI cutoff to use when classifying species, for each increment of the CGASI  
615 species cutoff, plotted on the x-axis, the percentage of intraspecies and interspecies comparisons  
616 correctly assigned was determined based on classically defined species designations. The ideal cutoff  
617 should maximize the prediction of classically defined species for both interspecies and intraspecies  
618 comparisons. The ANI-equivalent CGASI species cutoff is represented by the blue dotted line while the  
619 dDDH-equivalent CGASI species cutoff is represented by the red dotted line.

620 **Figure 3: Analysis of the ANI, dDDH, and CGASI values of 69 *Rickettsia* genomes**

621 For 69 *Rickettsia* genomes, **(A)** the ANI and dDDH values and **(B)** CGASI values were calculated for each  
622 genome comparison and color-coded to illustrate the results with respect to cutoffs of ANI  $\geq 95\%$  and  
623 dDDH  $\geq 70\%$ . The color of the shape represents species designations as determined by a CGASI cutoff  
624  $\geq 96.8\%$ . **(C)** A ML phylogenomic tree with 1000 bootstraps was generated using the core genome with  
625 bootstrap support values placed next to their corresponding nodes. **(D)** The relationships in the green  
626 box on Panel C cannot be adequately visualized at the necessary scale, so they are illustrated separately  
627 with a different scale. In all panels, the shape next to each *Rickettsia* genome represents whether the  
628 genome originates from an ancestral (●), transitional (◆), typhus group (▲), or spotted fever group (■)  
629 *Rickettsia* species.

630 **Figure 4: Analysis of the ANI, dDDH, and CGASI values of 16 *Ehrlichia* genomes**

631 For 16 *Ehrlichia* genomes, **(A)** the ANI and dDDH values and **(B)** CGASI values were calculated for each  
632 genome comparison and color-coded to illustrate the results with respect to cutoffs of ANI  $\geq 95\%$  and  
633 dDDH  $\geq 70\%$ . The color of the shape represents species designations as determined by a CGASI cutoff  
634  $\geq 96.8\%$ . **(C)** A ML phylogenomic tree with 1000 bootstraps was generated using the core genome with  
635 bootstrap support values placed next to their corresponding nodes.

636 **Figure 5: Analysis of the ANI, dDDH, and CGASI values of 30 *Anaplasma* genomes**

637 **(A)** For 30 *Anaplasma* genomes, the ANI and dDDH values were calculated for each genome comparison  
638 and color-coded to illustrate the results with respect to cutoffs of ANI  $\geq 95\%$  and dDDH  $\geq 70\%$ . When  
639 attempting to construct a core genome alignment using all 30 *Anaplasma* genomes, only a 20-kbp  
640 alignment was generated, accounting for  $<1\%$  of the average *Anaplasma* genome size. Therefore, CGASI  
641 values were calculated after the *Anaplasma* genomes were split into two subsets containing **(B)** twenty  
642 *A. phagocytophilum* genomes, and **(C)** the remaining ten *Anaplasma* genomes. Two phylogenomic trees  
643 were generated using the core genome alignments from **(D)** 20 *A. phagocytophilum* genomes and **(E)**

644 the remaining ten *Anaplasma* genomes. In all panels, the shape next to each genome denotes genus  
645 designations as determined by CGASI while the color of the shape denotes the species as defined by a  
646 CGASI cutoff of  $\geq 96.85\%$ .

647 **Figure 6: Analysis of the ANI, dDDH values of 23 *Wolbachia* genomes and CGASI values of 22  
648 *Wolbachia* genomes**

649 For 23 *Wolbachia* genomes, **(A)** The ANI and dDDH values and **(B)** CGASI values were calculated for each  
650 genome comparison and color-coded to illustrate the results with respect to cutoffs of ANI  $\geq 95\%$  and  
651 dDDH  $\geq 70\%$ . **(C)** A ML phylogenomic tree was generated using the *Wolbachia* core genome alignment  
652 constructed using 22 *Wolbachia* genomes. The species designations in supergroup B show the CGASI-  
653 designated species cluster of *wPip\_Pel*, *wPip\_JHB*, *wAus*, and *wStri* to be polyphyletic, indicating the  
654 need for amendments to the CGASI species criteria. In all panels, the shape denotes the current  
655 supergroups A (●), B (▲), C (■), D (◆), E (●), F (●) and L (◆) and the color denotes the species as  
656 defined by a CGASI cutoff of  $\geq 96.85\%$ .

657 **TABLES**658 **Table 1: Rickettsiales genome and core genome alignment statistics**

Genus	Family	Class	Genomes Analyzed	Established Species Represented	Average Genome Size (Mbp)	Core Genome Alignment Size (Mbp)	Percentage Core Genome Composition	Minimum CGASI
<i>Rickettsia</i>	Rickettsiaceae	Alphaproteobacteria	69	27	1.32	0.56	42.4%	81.7%
<i>Orientia</i>	Rickettsiaceae	Alphaproteobacteria	3	1	2.04	0.97	47.5%	96.3%
<i>Ehrlichia</i>	Anaplasmataceae	Alphaproteobacteria	16	4	1.23	0.49	39.8%	81.6%
<i>Neohellichia</i>	Anaplasmataceae	Alphaproteobacteria	1	1	1.27	NA	NA	NA
With <i>Ehrlichia</i>			17	5	1.24	0.11	8.9%	80.1%
<i>Anaplasma</i>	Anaplasmataceae	Alphaproteobacteria	30	3	1.39	0.02	1.4%	84.0%
<i>A. phagocytophilum</i>			20	1	1.5	1.25	83.3%	98.9%
<i>A. marginale</i> and <i>A. centrale</i>			10	2	1.18	0.77	65.3%	90.6%
<i>Neorickettsia</i>	Anaplasmataceae	Alphaproteobacteria	4	3	0.87	0.02	2.3%	85.7%
Excluding <i>N. helminthoeca</i> Oregon			3	2	0.87	0.76	87.4%	85.7%
<i>Wolbachia</i>	Anaplasmataceae	Alphaproteobacteria	23	NA	1.22	0.18	14.8%	77.2%
Excluding wPpe			22	NA	1.23	0.54	43.9%	80.1%
<i>Arcobacter</i>	Campylobacteraceae	Epsilonproteobacteria	44	12	2.27	0.43	18.9%	78.9%
<i>Caulobacter</i>	Caulobacteraceae	Alphaproteobacteria	26	4	4.97	1.61	32.4%	82.5%
<i>Erwinia</i>	Enterobacteriaceae	Gammaproteobacteria	22	10	4.42	0.60	13.6%	78.8%
<i>Neisseria</i>	Neisseriaceae	Betaproteobacteria	66	10	2.24	0.33	14.7%	80.5%
<i>Polaribacter</i>	Flavobacteriaceae	Flavobacteria	24	11	3.55	0.80	22.5%	77.9%
<i>Ralstonia</i>	Burkholderiaceae	Betaproteobacteria	21	3	5.44	1.24	22.8%	82.2%
<i>Thermus</i>	Thermaceae	Deinococci	19	11	2.29	1.10	48.0%	80.9%

659 **SUPPLEMENTARY FIGURE LEGENDS**

660 **Supplementary Figure 1: Assessing substitution saturation for core genome alignments**

661 For each of the 14 core genome alignments that comprise  $\geq 10\%$  of the average input genome size, the

662 uncorrected genetic distance between each of the members was plotted against the TN69-model

663 corrected genetic distance. The red-line represents the best-fit line for each data set while the black,

664 dotted-line represents the identity line ( $y=x$ ). In all cases, the relationship between the two distances are

665 linear ( $r^2 > 0.995$ ), indicating little substitution saturation in the core genome alignments.

666 **Supplementary Figure 2: Analysis of the ANI, dDDH, and CGASI values of three *Orientia* genomes**

668 For 3 *Orientia tsutsugamushi* genomes, **(A)** the ANI and dDDH values and **(B)** CGASI values were

669 calculated for each genome comparison and color-coded to illustrate the results with respect to cutoffs

670 of ANI  $\geq 95\%$  and dDDH  $\geq 70\%$ . Circles of the sample colors next to the names of each genome indicate

671 members of the same species as defined by a CGASI  $\geq 96.8\%$ .

672 **Supplementary Figure 3: Analysis of the ANI, dDDH, and CGASI of 4 *Neorickettsia* genomes**

673 **(a)** For the 4 *Neorickettsia* genomes, the ANI and dDDH values were calculated for each genome

674 comparison and color-coded to illustrate the results with respect to cutoffs of ANI  $\geq 95\%$  and dDDH

675  $\geq 70\%$ . **(b)** CGASI values were calculated and are illustrated using a core genome alignment that could

676 only be constructed using 3 of the *Neorickettsia* genomes, excluding *N. helminthoeca* Oregon. Circles of

677 the sample colors next to the names of each genome indicate members of the same species as defined

678 by a CGASI  $\geq 96.8\%$ .

679 **Supplementary Figure 4: Analysis of the ANI, dDDH, and CGASI of 66 *Neisseria* genomes**

680 For the 66 *Neisseria* genomes, **(A)** the ANI and dDDH values and **(B)** CGASI values were calculated for

681 each genome comparison and color-coded to illustrate the results with respect to cutoffs of ANI  $\geq 95\%$

682 and dDDH  $\geq 70\%$ . **(c)** A ML phylogenomic tree was generated using 1,000 bootstraps with the 0.33 Mbp

683 *Neisseria* core genome alignment. Circles of the sample colors next to the names of each genome  
684 indicate members of the same species as defined by a CGASI  $\geq 96.8$

685 **SUPPLEMENTARY TABLES**

686 **Supplementary Table 1: Genomes used for ANI, dDDH, and CGASI analysis**

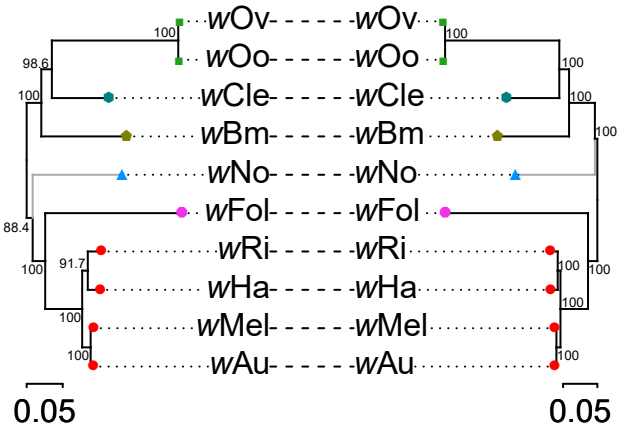
687 **Supplementary Table 2: ANI, dDDH, and CGASI values for 7,264 interspecies comparisons of**  
688 **the *Rickettsia*, *Orientia*, *Ehrlichia*, *Anaplasma*, *Neorickettsia*, *Wolbachia*, *Arcobacter*,**  
689 ***Caulobacter*, *Erwinia*, *Neisseria*, *Polaribacter*, *Ralstonia*, and *Thermus* genera**

690 **Supplementary Table 3: ANI, dDDH, and CGASI values for 100 intraspecies comparisons with a**  
691 **CGASI  $< 97.6\%$**

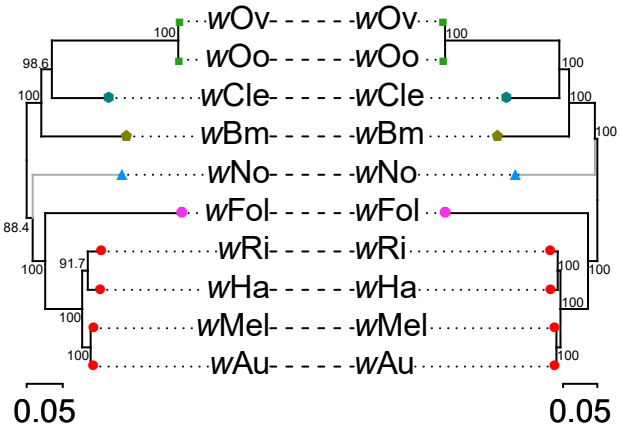
692 **Supplementary Table 4: ANI, dDDH, and CGASI values for 41 intraspecies comparisons with a**  
693 **CGASI  $< 96.8\%$**

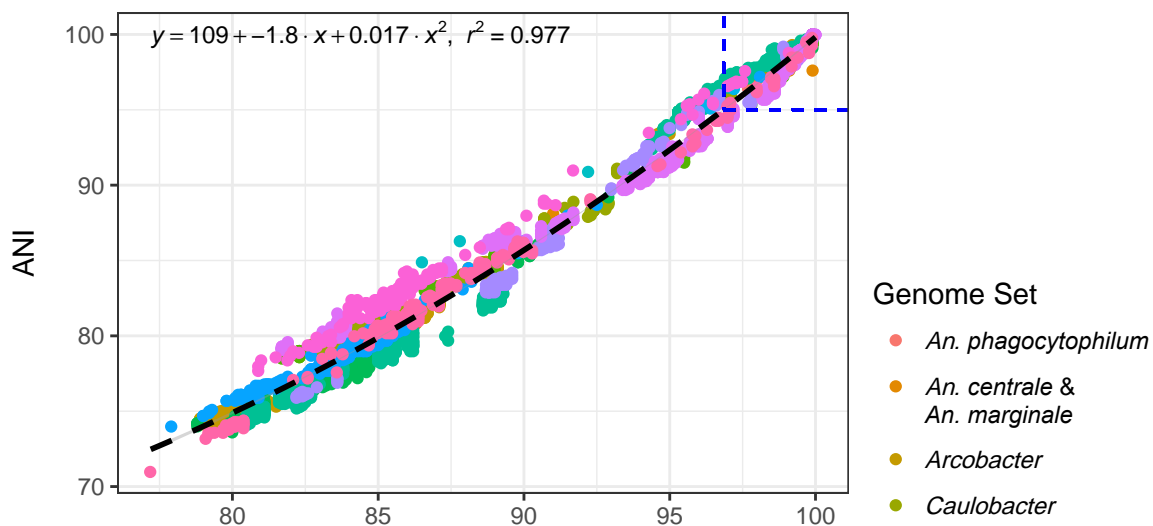
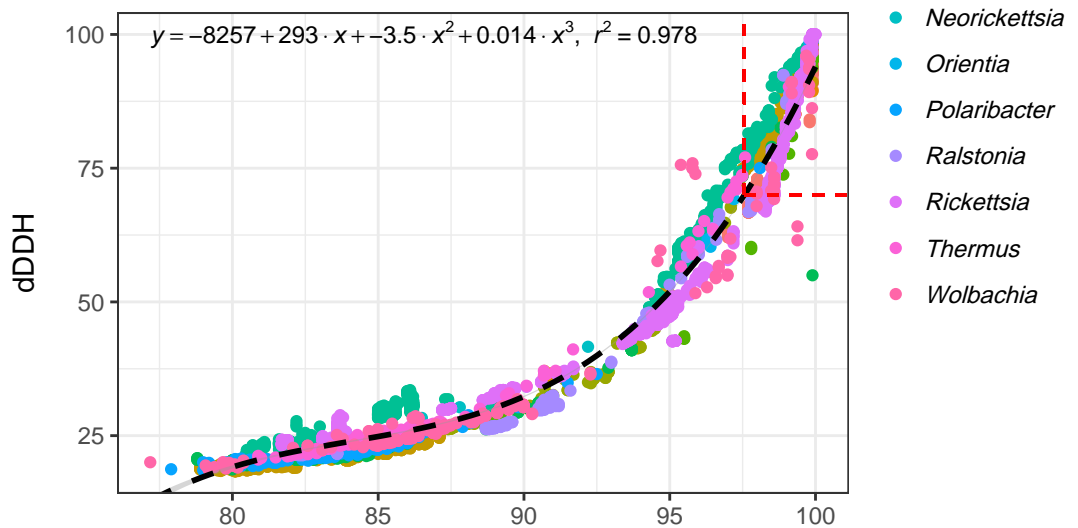
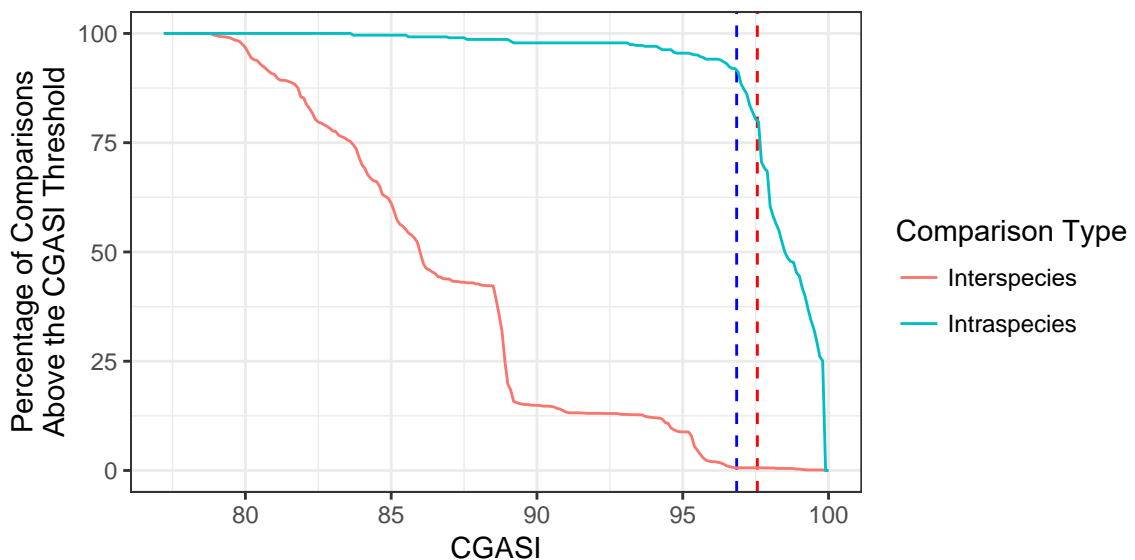
694 **Supplementary Table 5: ANI, dDDH, and CGASI values for 10 non-*Rickettsia* interspecies**  
695 **comparisons determined to be intraspecies using the ANI-derived CGASI cutoff of 96.8%**

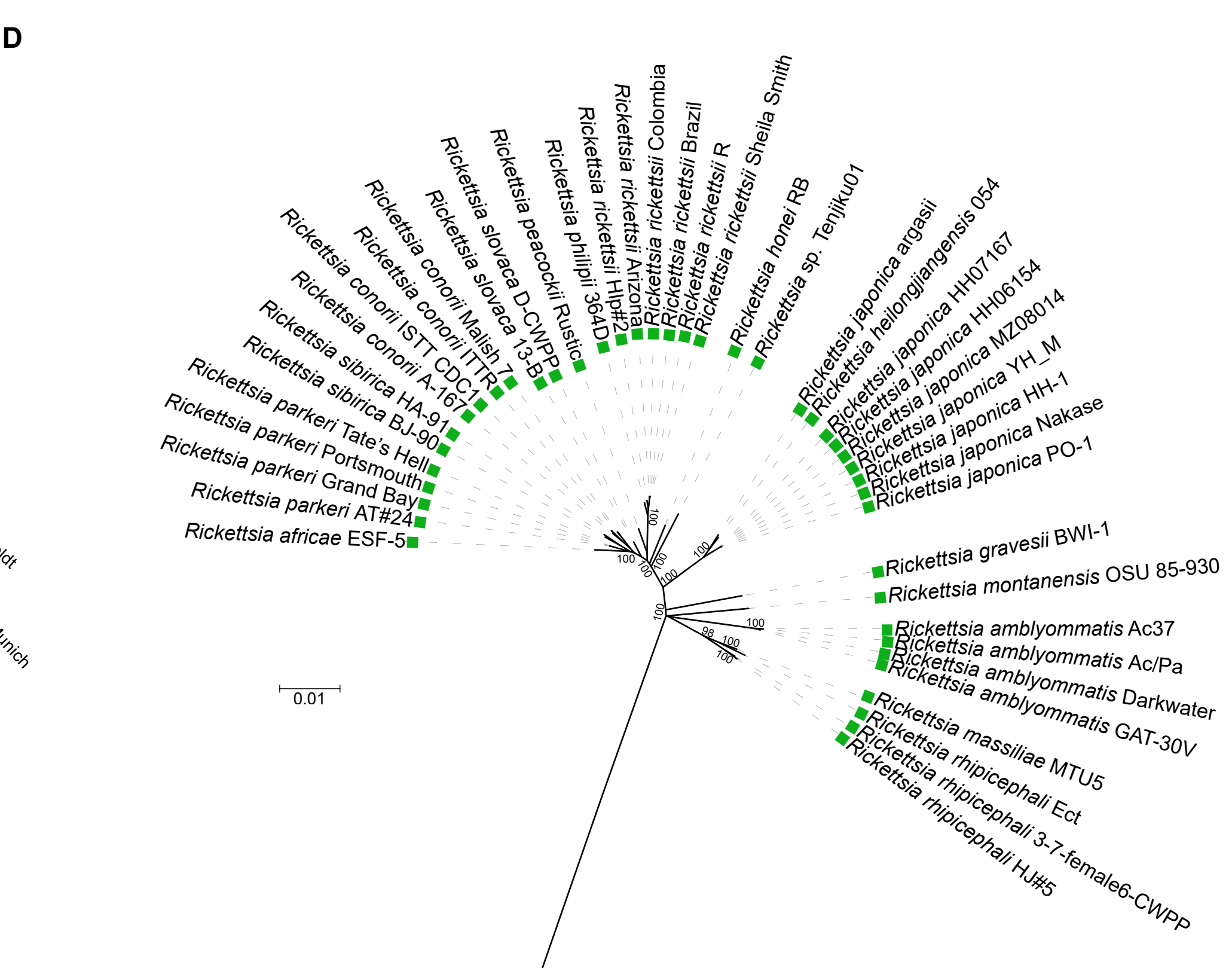
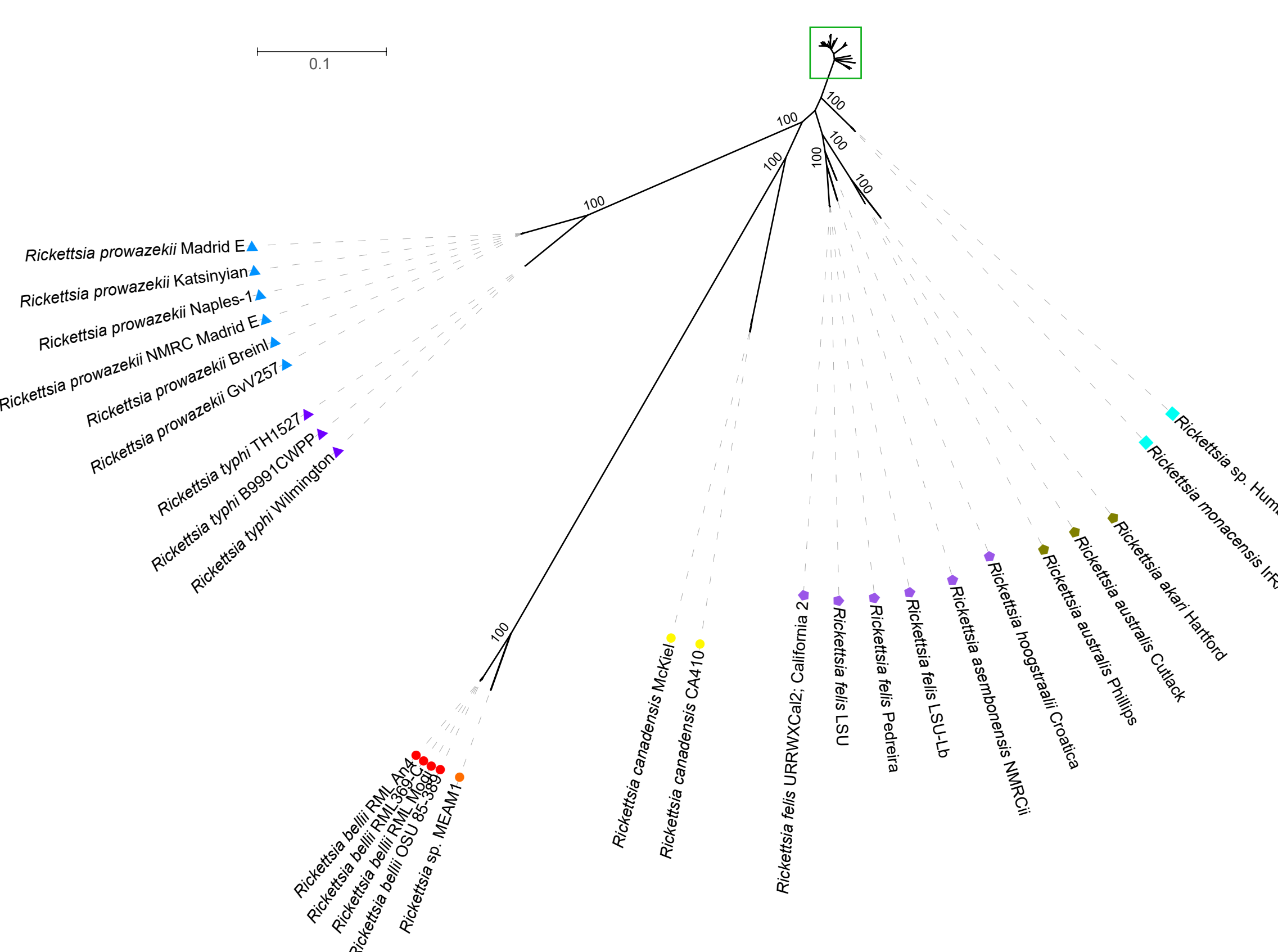
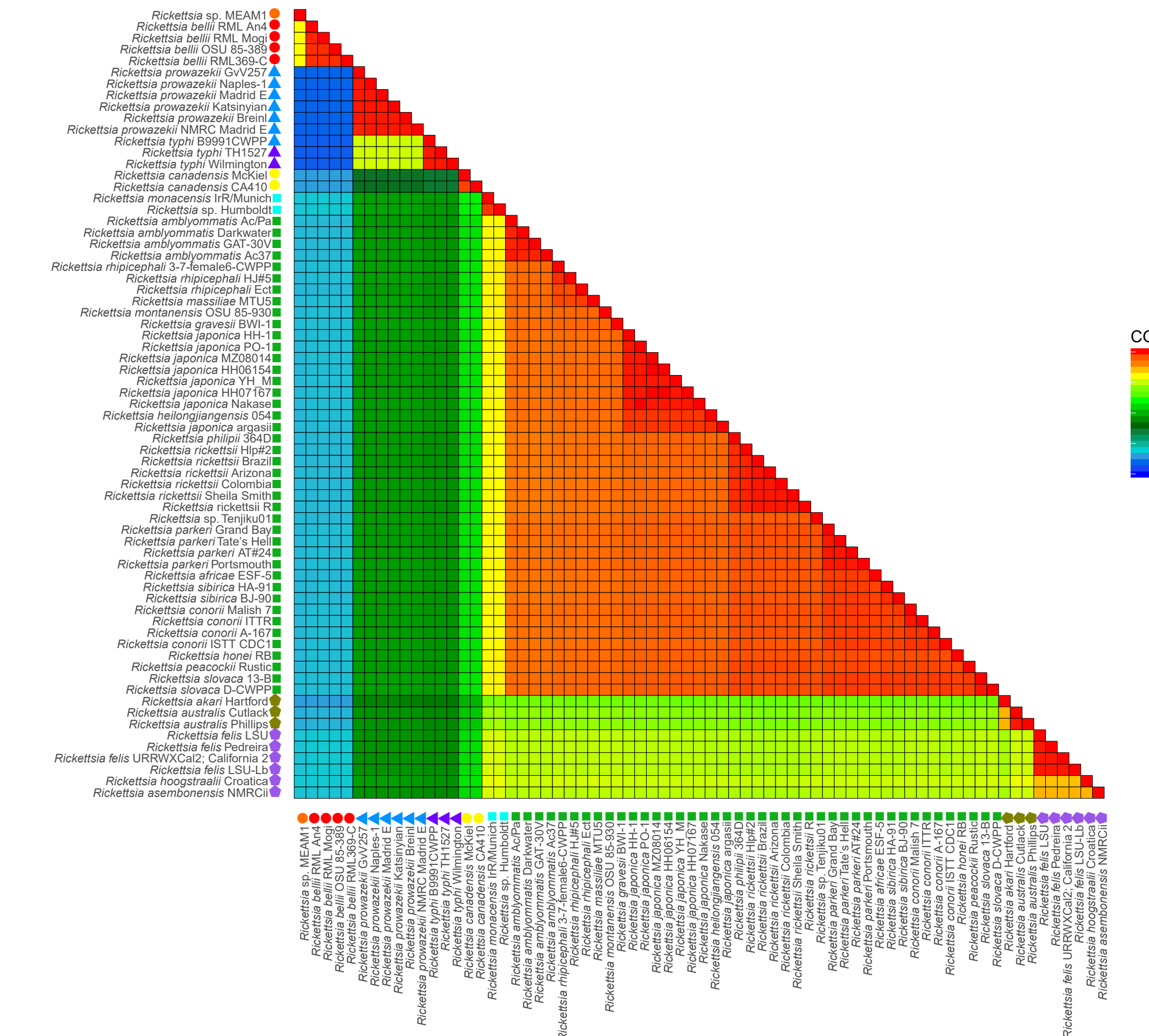
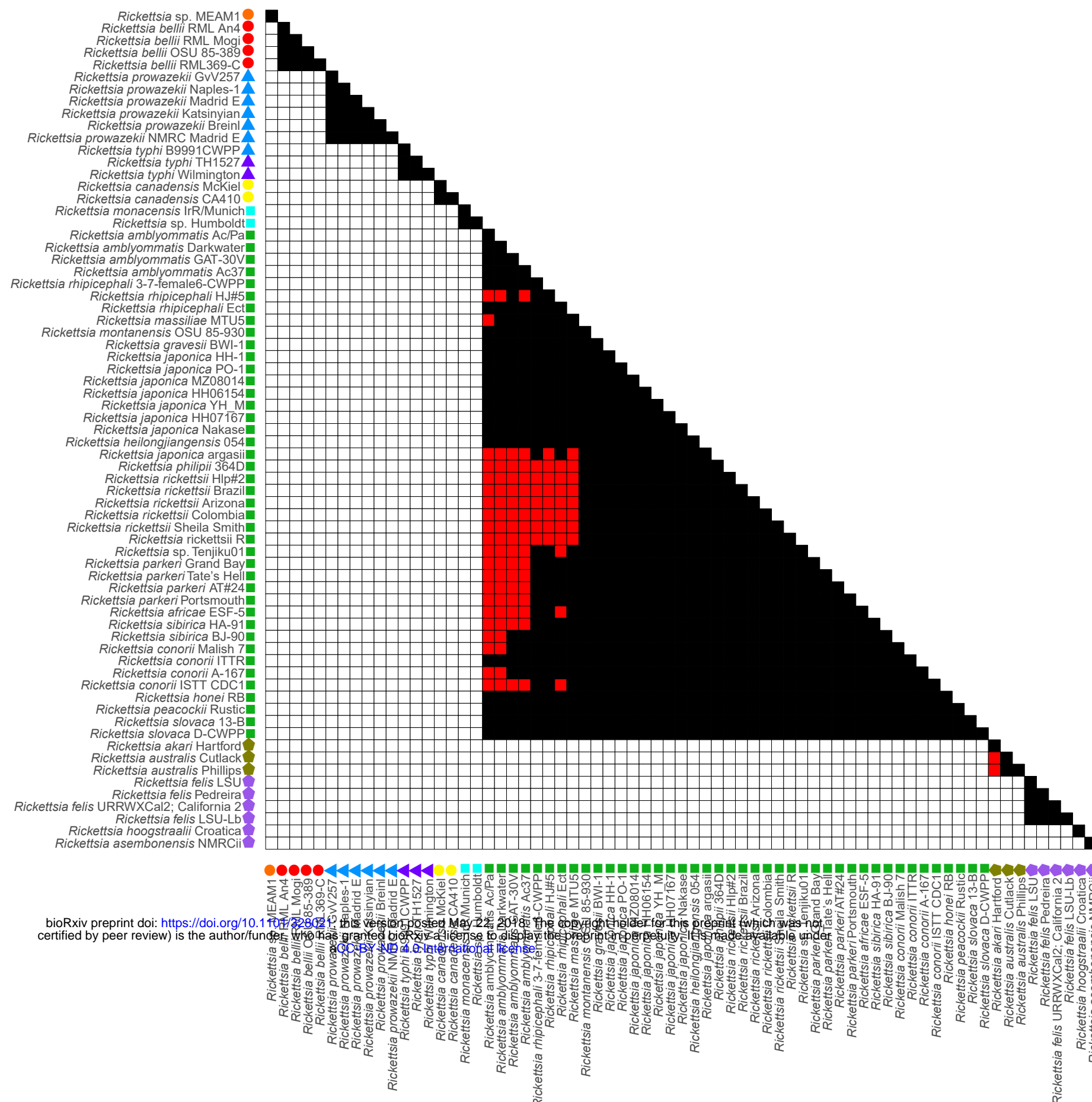
# A. CPA

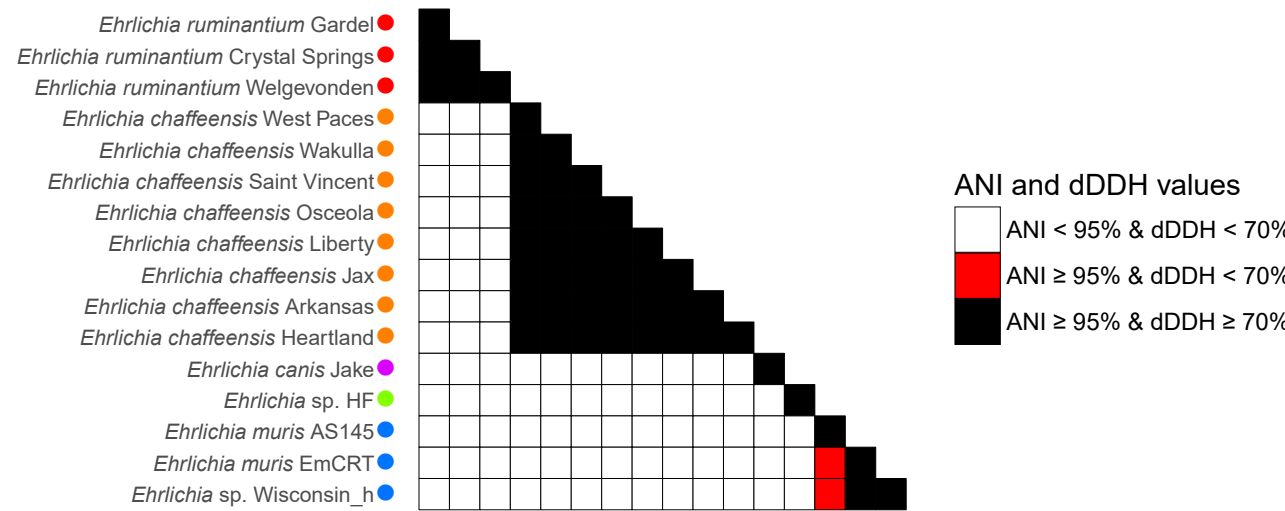
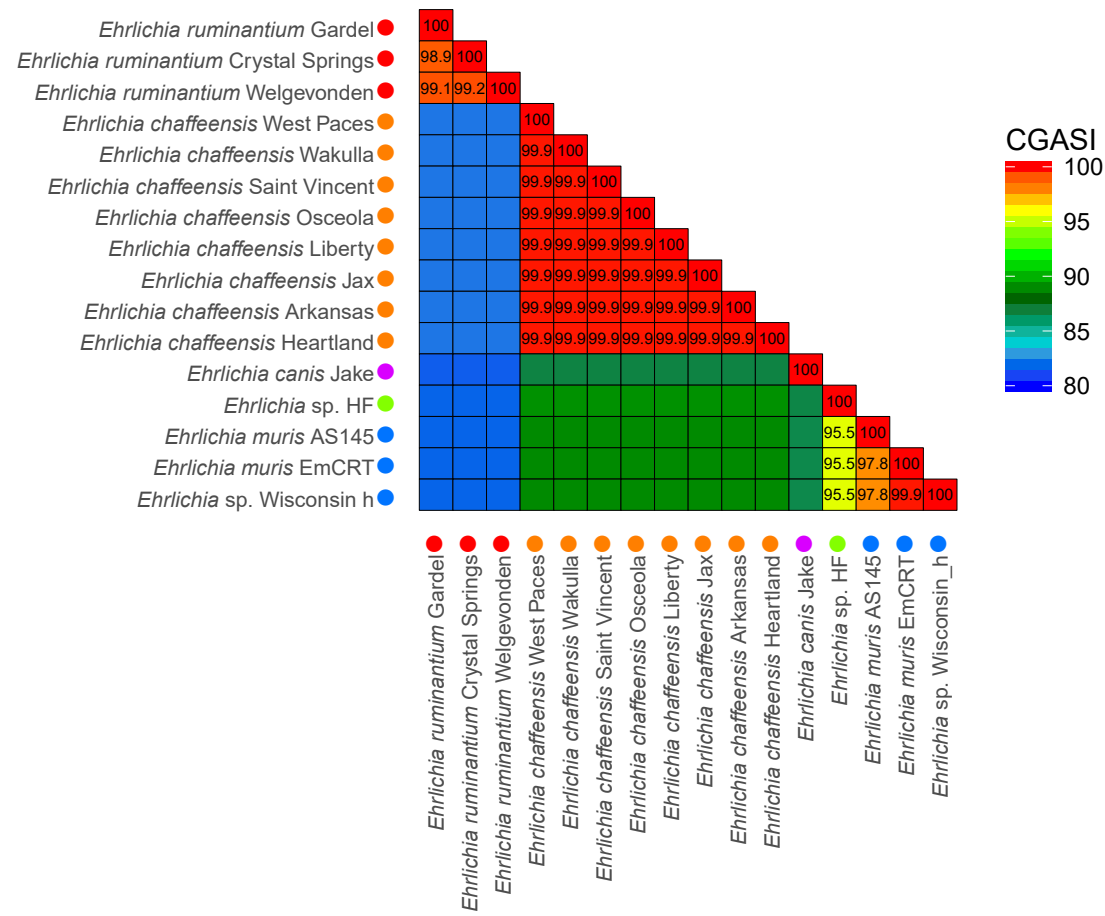
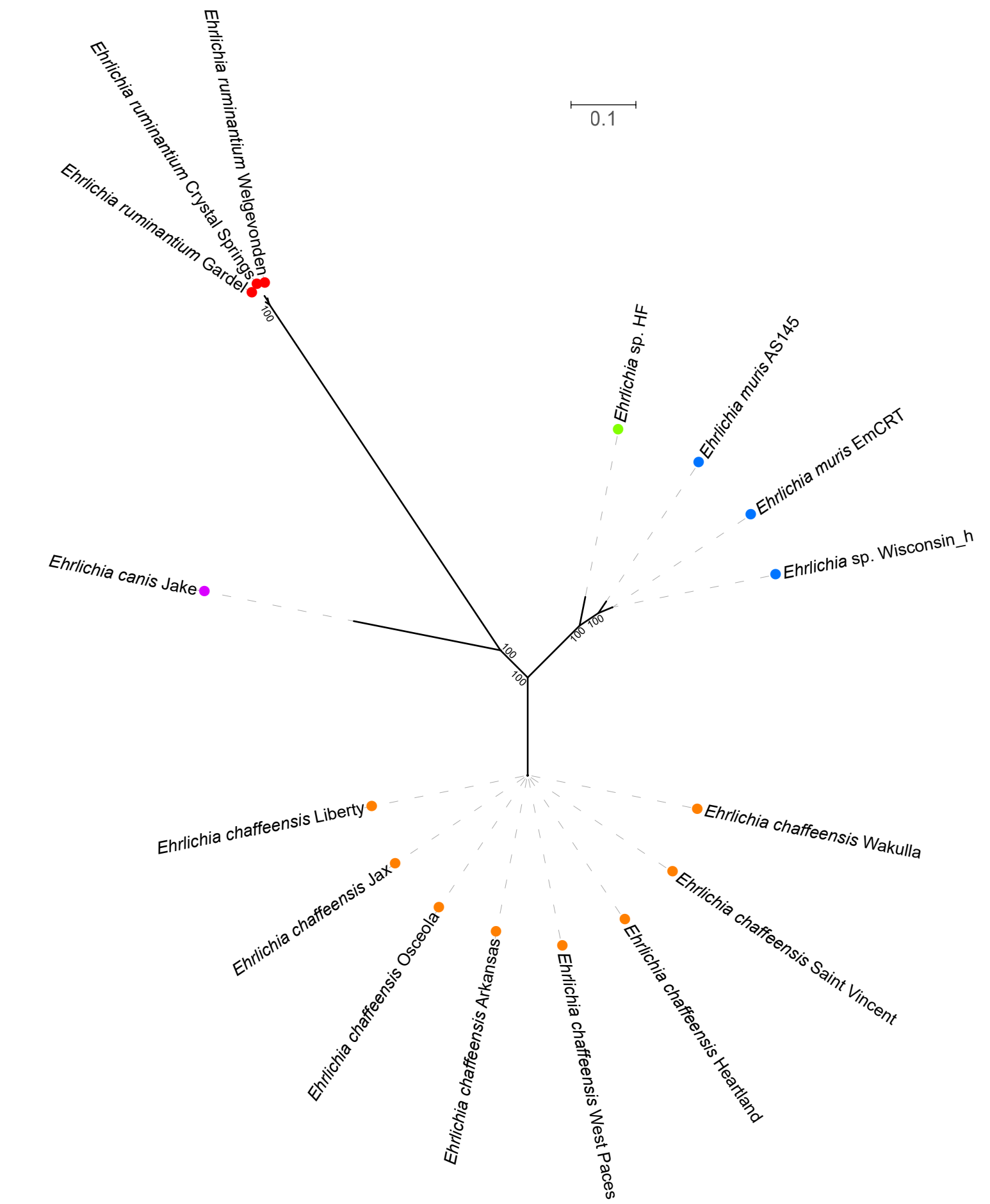


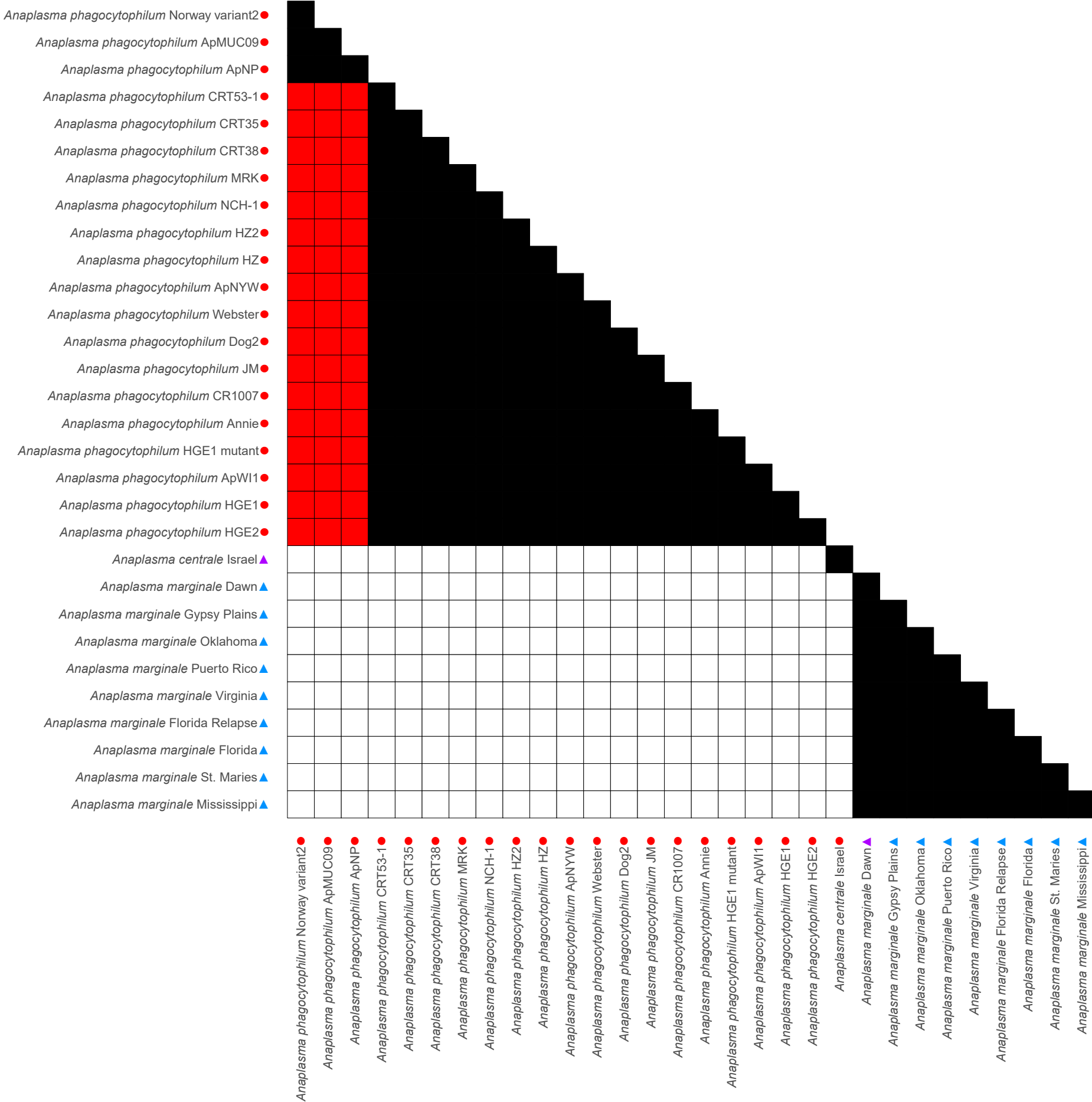
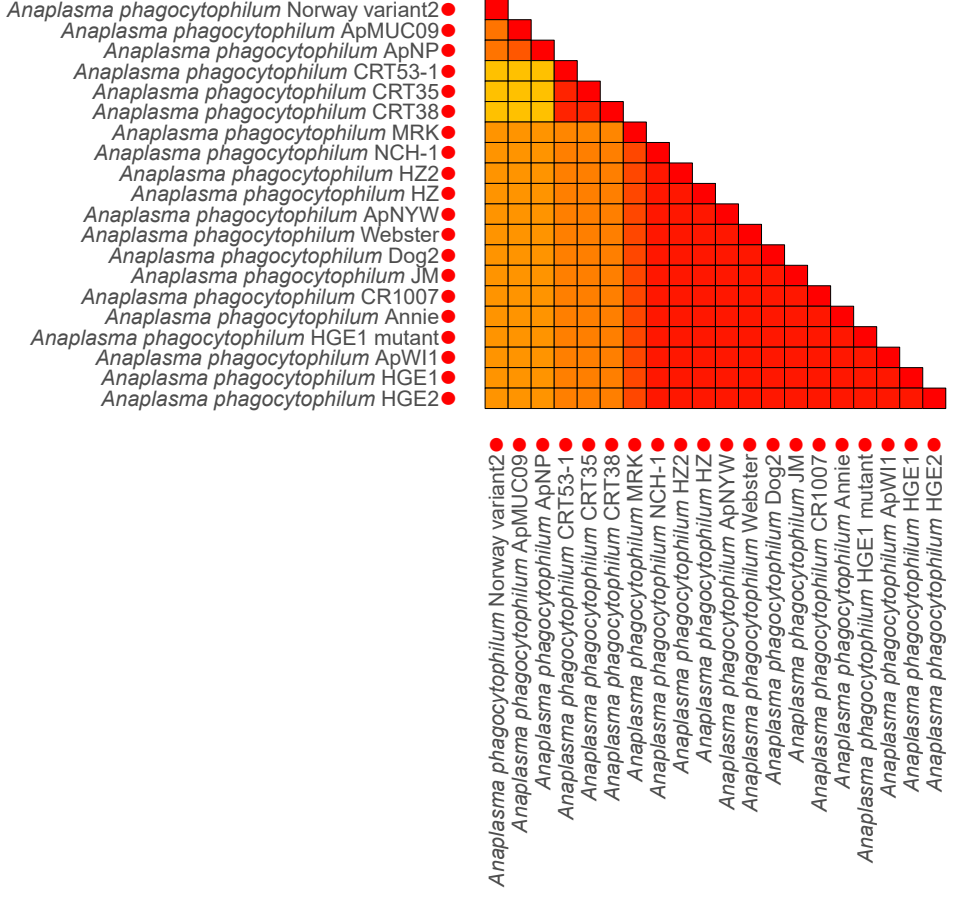
# B. CGA



**A****B****C**



**A****B****C**

**A****B****C**